CORTEX 78 (2016) 15–30

Available online at www.sciencedirect.com

ScienceDirect

Journal homepage: www.elsevier.com/locate/cortex

Clinical neuroanatomy

Importance of human right inferior frontoparietal network connected by inferior branch of superior longitudinal fasciculus tract in corporeal awareness of kinesthetic illusory movement

Kaoru Amemiya [a,b,c] *and Eiichi Naito* [c,d,*]

[a] *The Japan Society for the Promotion of Science, Tokyo, Japan*
[b] *Department of Biosciences and Informatics, Faculty of Science and Technology, Keio University, Yokohama, Kanagawa, Japan*
[c] *Center for Information and Neural Networks (CiNet), National Institute of Information and Communications Technology (NICT), Suita, Osaka, Japan*
[d] *Graduate School of Medicine & Graduate School of Frontier Biosciences, Osaka University, Suita, Osaka, Japan*

ARTICLE INFO

Article history:
Received 24 May 2015
Reviewed 16 October 2015
Revised 14 December 2015
Accepted 18 January 2016
Action editor Marco Catani
Published online 17 February 2016

Keywords:
Kinesthetic illusion
Motor imagery
Superior longitudinal fasciculus
Right frontoparietal cortices
Corporeal awareness

ABSTRACT

It is generally believed that the human right cerebral hemisphere plays a dominant role in corporeal awareness, which is highly associated with conscious experience of the physical self. Prompted by our previous findings, we examined whether the right frontoparietal activations often observed when people experience kinesthetic illusory limb movement are supported by a large-scale brain network connected by a specific branch of the superior longitudinal fasciculus fiber tracts (SLF I, II, and III).

We scanned brain activity with functional magnetic resonance imaging (MRI) while nineteen blindfolded healthy volunteers experienced illusory movement of the right stationary hand elicited by tendon vibration, which was replicated after the scanning. We also scanned brain activity when they executed and imagined right hand movement, and identified the active brain regions during illusion, execution, and imagery in relation to the SLF fiber tracts.

We found that illusion predominantly activated the right inferior frontoparietal regions connected by SLF III, which were not substantially recruited during execution and imagery. Among these regions, activities in the right inferior parietal cortices and inferior frontal cortices showed right-side dominance and correlated well with the amount of illusion (kinesthetic illusory awareness) experienced by the participants.

The results illustrated the predominant involvement of the right inferior frontoparietal network connected by SLF III when people recognize postural changes of their limb. We assume that the network bears a series of functions, specifically, monitoring the current

* *Corresponding author*. Center for Information and Neural Networks (CiNet), National Institute of Information and Communications Technology (NICT), 2A6, 1-4 Yamadaoka, Suita, Osaka, 565-0871, Japan.
E-mail address: eiichi.naito@nict.go.jp (E. Naito).

http://dx.doi.org/10.1016/j.cortex.2016.01.017

status of the musculoskeletal system, and building-up and updating our postural model (body schema), which could be a basis for the conscious experience of the physical self.

1. Introduction

The human cerebral cortex is composed of two distinct (right and left) hemispheres and each hemisphere appears to exhibit bilateral asymmetry, but not complete asymmetry, in both structure and function. The typical example is language lateralization to the left 'dominant' hemisphere (Binder et al., 1997; Catani et al., 2007; Springer et al., 1999; Wada & Rasmussen, 2007). Yet, lateralization of the right 'non-dominant' hemisphere is still less understood.

There is ample neuropsychological evidence suggesting that a variety set of frontoparietal brain regions in the right hemisphere plays crucial roles in the formation of the internal representation of one's body, which is highly associated with the conscious experience of physical self (corporeal awareness: Berlucchi & Aglioti, 1997; Daprati, Sirigu, & Nico, 2010; Melzack, 1990). In favor of this view, we have shown that right inferior frontal cortices (cytoarchitectonic areas 44 and 45) and inferior parietal lobules (supramarginal gyrus, cytoarchitectonic areas PF and its subregions) dominantly activate in the right hemisphere when right-handed healthy people experience illusory limb movement elicited by muscle afferent input from a vibrated limb (Naito et al., 2007, 2005). However, it remains unclear whether these right inferior frontoparietal activations during corporeal awareness of illusory limb movement are supported by a large-scale brain network connected by a specific brain fiber tract.

In human neuroimaging literature, it has been demonstrated that superior longitudinal fasciculus (SLF) fiber tracts that connect a broader range of the frontoparietal regions are composed of three branches (SLF I-III; Makris et al., 2005; Rojkova et al., in press; Thiebaut de Schotten et al., 2011; Thiebaut de Schotten, Dell'Acqua, Valabregue, & Catani, 2012). Among these fiber tracts, the inferior branch (SLF III) appears to connect a wide range of inferior frontoparietal cortices including higher-order somatosensory and visual association cortices, inferior parietal cortices, inferior frontal cortices, ventrolateral prefrontal cortices, and orbitofrontal cortices (Thiebaut de Schotten et al., 2011). Thus, it is highly likely that the right inferior frontoparietal cortices active during illusion belong to this large-scale inferior frontoparietal network connected by SLF III.

Another important question is whether, among various types of motor-related events (execution, imagery, and illusion), the right hemisphere dominance is confined to the illusion. Both execution and imagery are voluntary motor events where one is the agent of these events and the brain voluntarily generates and simulates motor commands (Daprati et al., 2010), while illusion is basically a bottom-up sensory (kinesthetic) event where motor intention and voluntary generation of motor commands are not particularly required. Thus, if the right inferior frontoparietal cortices are specialized to the formation of internal representation of one's body based on bottom-up sensory processing, one would expect substantial brain activity in the right inferior frontoparietal cortices only during illusion. Also important, if subjective experience of kinesthetic illusion is an attribute of neuronal activities that are associated with the formation of internal representation of one's body, we may expect that the right inferior frontoparietal activities would reflect the degree of kinesthetic illusory awareness.

In the present study, we scanned brain activity with functional magnetic resonance imaging (fMRI) while nineteen blindfolded healthy volunteers experienced illusory movement of the right stationary hand, which was elicited by muscle afferent input driven by tendon vibration (Goodwin, McCloskey, & Matthews, 1972; Roll & Vedel, 1982; Roll, Vedel, & Ribot, 1989). We also scanned brain activity when they executed and imagined right hand movement, and identified the brain regions active during illusion, execution, and imagery in relation to the SLF fiber tracts. We reported brain activation locations in relation to the brain regions connected by SLF fiber tracts and the cytoarchitectonic probability maps (Eickhoff et al., 2005).

2. Methods

2.1. Participants

Nineteen blindfolded right-handed (five female) volunteers with no history of neurological or psychiatric disease participated in the experiments. Their ages ranged from 20 to 38 years [average 23.7 ± 4.5 (SD)]. All participants provided their written informed consent and the study was approved by the ethical committee of Kyoto University. The fMRI experiment was carried out following the principles and guidelines of the Declaration of Helsinki (1975).

2.2. Behavioral experiment

Before we conducted the fMRI experiment, we performed a behavioral experiment in which the participants practiced exactly the same tasks (illusion, execution, and imagery of right hand movement) that were subsequently conducted in the following fMRI experiment. Another objective in this experiment was to evaluate electromyogram (EMG) activity during each task.

The participants lay comfortably on a bed in the supine position with their eyes closed. Both their right and left arms were naturally semi-pronated, extended in front of them, and fixed on a wooden apparatus (Fig. 1A) that was also used in the

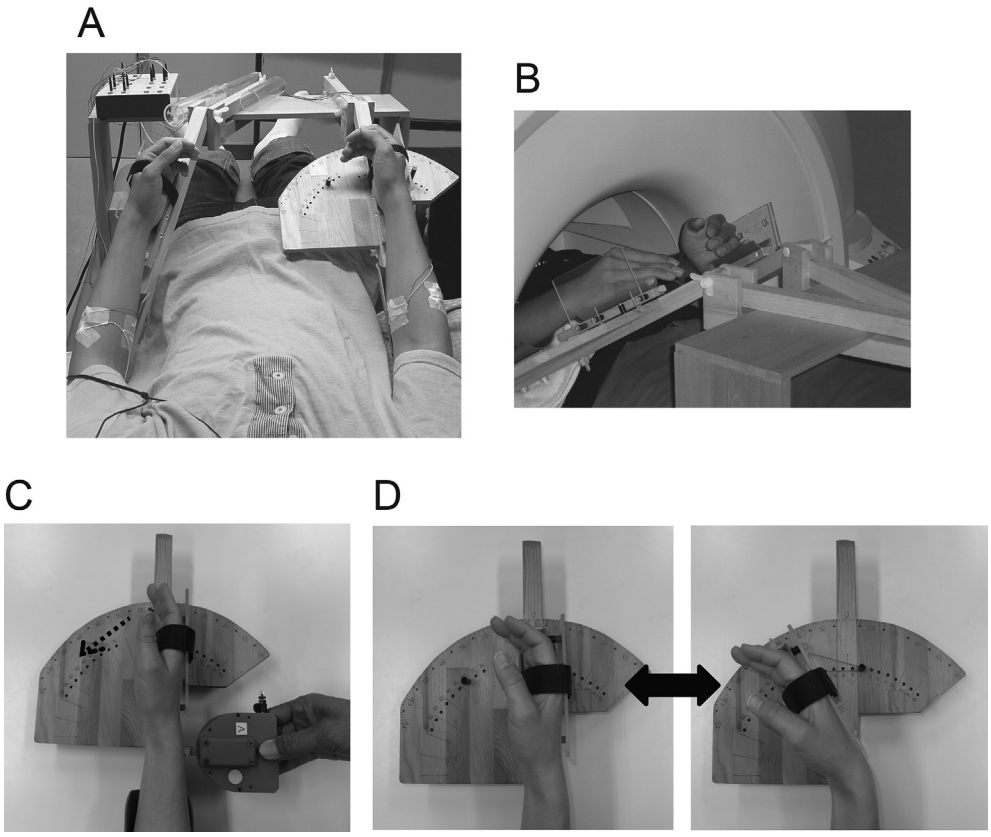

Fig. 1 – Experimental setup for EMG evaluation outside MRI scanner (A) and for MRI experiment (B). A: Both arms were supported by the apparatus. We recorded EMG activity during execution, imagery, and illusion tasks outside the scanner. B: The same apparatus was used in the fMRI scanner. C: Illusion task. In the tendon-vibration epoch, the right wrist was fixed in the natural straight (start) position and relaxed in this position. We vibrated the tendon of the ECU muscle of the right hand, which elicited illusory flexion of the stationary hand. After the session, the participants reported maximum illusory flexion angle by actually flexing their wrists, and we measured the angle using the protractor. D: Execution task. In the execution epoch, we asked the participants to flex (or extend) their right wrists in synchronization with a sound and to hold this position until the next sound. Thus, in the flexion phase, they had to generate a force against the rubber-band-generated resistance (approximately 250 g) and to keep generating the force to hold the 30-deg flexion position (right panel; An arrow indicates rubber band). In the extension phase, the contractile force of the rubber band assisted the movement and the participants could relax their wrists at the start position (left panel).

MR scanner (Fig. 1B). Their hands naturally straightened and each hand was affixed to the apparatus with a hook and loop fastener (Fig. 1A). In this situation, the participants could relax both arms and their whole body. Specifically, the right hand was fixated on a special device (Fig. 1C, D). A mobile indicator was mounted on the surface of this device and angular degrees were scaled as an ordinal protractor on its surface. We fixed the right hand on this mobile indicator so that the radiocarpal joint of the wrist was located just above the origin of the protractor. We defined the 0 ° of the wrist angle as the direction when the wrist became straight, as shown in Fig. 1C. By doing so, we could read the wrist angles when the participants moved their right wrists.

The behavioral experiment consisted of two sessions: a vibration session and an execution-imagery session. Each session was composed of nine experimental epochs. In the vibration session, the tendon-vibration, bone-vibration, or rest epoch was repeated three times. Likewise, in the execution-imagery session, the execution, imagery, or rest epoch was repeated three times. In both sessions, the order of each epoch was pseudo-randomized across participants, except that the imagery epoch was performed after the execution epoch (i.e., execution, imagery, rest or rest, execution, imagery or execution, rest, imagery) in the execution-imagery session. Each epoch lasted 27 sec with an inter-epoch-interval of 6 sec. In each session, we also added 6 sec before each session started and another 6 sec after the last epoch finished. Eventually, each session lasted for 303 sec.

2.3. *Vibration session*

In the vibration session, the right wrists were fixed in the natural straight (start) position and relaxed in this position (Fig. 1C). In the tendon-vibration epoch, we vibrated the tendon of the extensor carpi ulnaris (ECU) muscle of the right hand for 27 sec (Fig. 1C). We expected the vibration to elicit illusory flexion of the right stationary hand. Likewise, in the bone-vibration epoch, we vibrated the skin surface over a nearby bone (i.e.,

the processus styloideus ulnae of the hand) for 27 sec. In the rest epoch, we did not provide any vibration stimuli and the participants relaxed their wrists in the start position. We know from our previous studies (Naito et al., 2007, 2005) that, in the bone-vibration epoch, most participants mainly feel vibration sensations without experiencing any reliable illusions. Thus, we used this as a cutaneous control for the tendon-vibration task. We used a non-magnetic vibrator (110 Hz; ILLUSOR, Umihira Ltd, Kyoto, Japan; Fig. 1C) driven by constant air pressure provided by an air-compressor (Naito et al., 2007). We used an amplitude (3.5 mm) of vibration stimuli that was identical in the fMRI scanning. The contact surface on the skin was approximately 1 cm^2 for the two vibration conditions. One experimenter (EN) operated the vibrator by manually applying it to the skin with light pressure. Computer-generated visual cues were given to the experimenter in order to instruct him to start and stop tendon-vibration, bone-vibration, and rest epochs. The participants could not see these cues.

In this session, we asked the participants to relax their hands and arms to prevent limb movement, and to be aware of movement sensation from the vibrated hand. They were also asked to remember the maximum illusory flexion angle if they experienced sensation. To confirm if they experienced an illusion during vibration, after the onset of vibration stimuli when they started feeling illusory movement, the participants were asked to say 'start' and, if the illusions disappeared within 27 sec, they were asked to say 'stop.' (This was not allowed in the MRI scanner.)

After the end of the session, we asked them if they experienced the illusion. Since none of the participants experienced any reliable illusions in the bone-vibration epochs, they only replicated the illusory movement experienced in the tendon-vibration epochs. For the replication, they flexed their right wrists until they showed the maximum illusory flexion angle. They had to replicate their remembered angles for each of the three tendon-vibration epochs. We measured these angles from the relaxed position with the protractor (Fig. 1A). Then, we calculated the mean maximum illusory angle across three epochs for each participant (Fig. 2C).

2.4. *Execution-imagery session*

In this session, except for the rest epoch, the participants executed (execution) or imagined (imagery) their right hand movements in synchronization with computer-generated sounds provided through a headphone. A sound was provided every 2 sec. We selected this movement frequency because, in our pilot experiment, we found that some people had difficulty imagining the movements as if they actually performed them when the frequency was higher than this. In the rest epoch, they also heard these sounds, but they were asked to relax their hands without producing any movement. Each task (execution, imagery, or rest) to be performed in the next epoch was verbally instructed 3.5 sec prior to each epoch. We also gave the participants auditory instructions of "3, 2, 1, start" to provide the exact start of each epoch and "stop" to provide the exact cessation of each epoch. All of these were also generated by the computer.

In the execution epoch, the participants either flexed or extended their right wrists in synchronization with a sound and repeated this task for 27 sec. In this epoch, we fixated two stoppers on the protractor device in order to control the range of wrist motion across trials and participants (Fig. 1D). One was fixated at the start position in order to prevent the wrist from extending beyond the straight (0 °) position. The other was prepared in order to prevent the wrist from flexing beyond 30 ° of flexion. This angle was selected because we know from our pilot experiment that the mean maximum illusory flexion angle was about 30° across the present participants (Supplementary Fig. 1A) and we wanted the participants to generate a comparable amount of wrist flexion. We also set a rubber band to connect between the mobile indicator and the stopper on the start position (Fig. 1D). In the execution epoch, we asked the participants to flex (or extend) their right wrists in synchronization with a sound and to hold this position until the next sound. Thus, in the flexion phase, they had to generate a force against the rubber-band-generated resistance (approximately 250 g) and to keep generating the force to hold the 30-deg flexion position (Fig. 1D right panel). However, in the extension phase, the contractile force of the rubber band could assist the movement and the participants could relax their wrists at the start position (Fig. 1D left panel). These were done because, in the tendon-vibration epoch, we could expect that the participants would experience illusory flexion movement of the right wrist and we wanted to evaluate the EMG activity when the participants emphasized the flexion phases of their wrist movements.

In the imagery epoch, we asked them to imagine a first-person perspective, kinesthetic motor imagery where they mentally simulate the movements as if they actually performed exactly the same wrist movements they produced in a corresponding previous execution epoch (Naito, Kochiyama, et al., 2002). We also gave them an instruction not to generate any actual movements. After the execution-imagery session, we asked the participants if they could imagine the first-person perspective, kinesthetic motor imagery. All of them reported that they could do so.

In our pilot experiment before the behavioral experiment, we evaluated how vividly each participant could imagine first-person perspective, kinesthetic motor imagery. In our previous study (Naito, Kochiyama, et al., 2002), we showed that, when we asked the participants to additionally imagine that the right hand with illusory flexion was flexing further, motor imagery can augment the illusory experience in persons who have a higher ability to control kinesthetic motor imagery, which was evaluated by the controllability of motor imagery (CMI) test (Naito, 1994). The motor imagery of persons who score lower in the CMI test (poor at having kinesthetic motor imagery) tends to disturb the illusory flexion experience so as to reduce the amount of illusion when compared with the case of without imagery. Thus, if the motor imagery of wrist flexion in the present participants augments the illusory wrist flexion, we may presume that their ability to have kinesthetic motor imagery is reliable and that they are likely to have vivid kinesthetic imagery during the imagery epochs. Based on this assumption, we prepared four 27-sec epochs; in two the participants merely experienced illusory flexion of the right wrist without having imagery and, in the other two, they additionally imagined that the right hand with illusory flexion was further flexing. After each epoch, they replicated the maximum illusory flexion angle

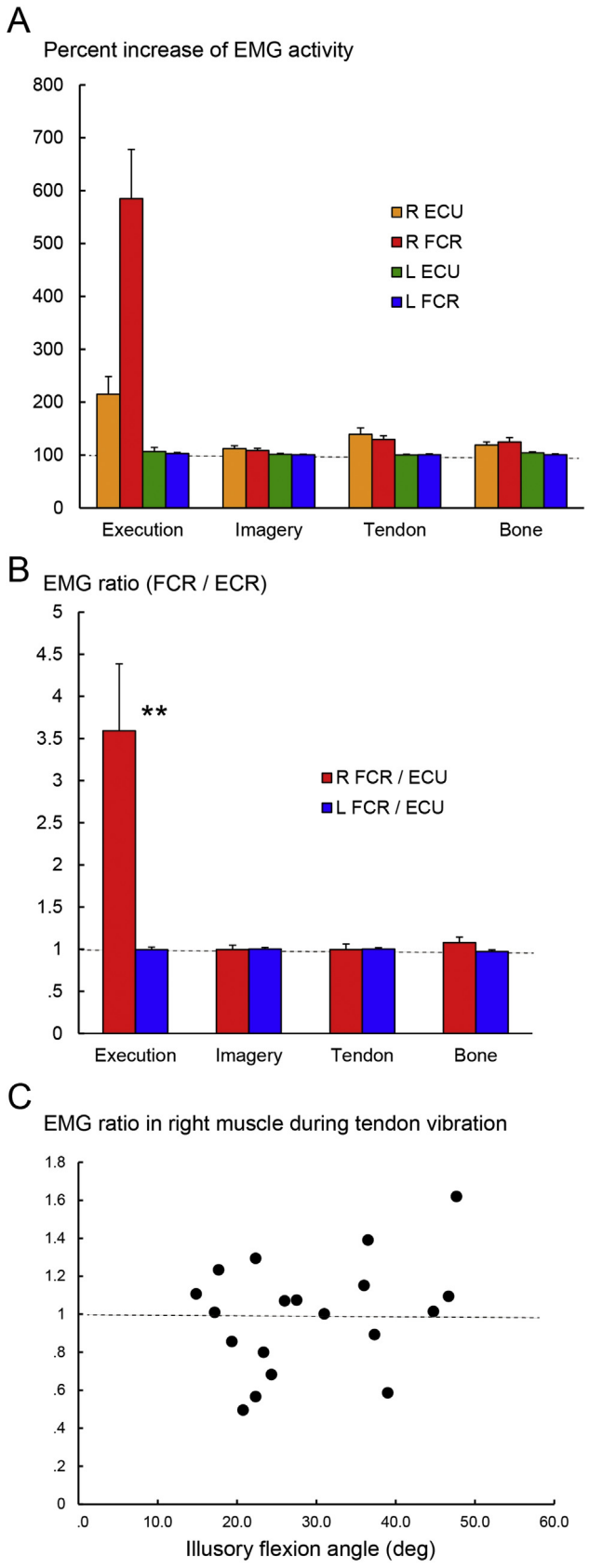

Fig. 2 – Results from behavioral experimental outside scanner. A: Percent increase of EMG activity in FCR and ECU muscles of right and left wrists during execution (leftmost), imagery (left), tendon-vibration (right), and bone-vibration (rightmost). Bars in different colors indicate the data obtained from each muscle (orange for right ECU, red for right FCR, green for left ECU, and blue for left FCR). Standard error of the mean across participants (SE) is shown on the top of each bar. B: EMG ratio showing prominence of FCR activity compared with ECU activity. Red bars represent right muscle data and blue bars indicate left muscle data. SE is shown on the top of each bar. C: Correlation between illusory flexion angle (horizontal axis) and EMG ratio in the right muscle during tendon vibration (vertical axis). Each dot represents the data obtained from each participant. The dotted line indicates EMG ratio = 1.

by actually flexing their wrists and we measured these angles. The mean maximum illusory flexion angle was calculated for each with and without imagery epochs, and the amount of illusion with imagery was divided by that without imagery (augmented ratio). We confirmed that motor imagery augmented the illusory experience in 16 participants (Supplementary Fig. 1A) and the mean augmented ratio across participants was 1.4 (range from .7 to 2.1; Supplementary Fig. 1B). Thus, the majority of the present participants appeared to have vivid and reliable kinesthetic motor imagery during the imagery epochs.

2.5. *EMG recording and analysis*

In both sessions, we recorded EMG from the skin surface over the ECU and the flexor carpi radialis (FCR) of both the right and left arms. A pair of 8-mm diameter Ag/AgCl electrodes (NT-211 U, Nihon Kohden, Tokyo, Japan) were placed on the skin surface over each muscle. The signals were amplified 2000 times using an amplifier (AB-610J, Nihon Kohden, Tokyo, Japan) and recorded using software (PowerLab/16SP, ADInstruments, Australia) for off-line analysis (Kito, Hashimoto, Yoneda, Katamoto, & Naito, 2006). In the analysis, EMG from each muscle was first rectified and the integrated EMG (iEMG) for 27 sec of each epoch was calculated for each participant. Then, each iEMG for execution, imagery, tendon-vibration, and bone-vibration epoch was normalized by the iEMG in their corresponding rest epoch (27 sec). Then, we calculated the mean normalized iEMG for each task (execution, imagery, tendon-vibration, and bone-vibration) across epochs for each participant. This procedure gave us the percent increase of EMG activity from the baseline EMG activity during rest for each muscle for each task separately. We list the mean EMG-activity percent increase in each muscle for each task across participants in Fig. 2A. Next, to evaluate the degree of prominence of the FCR activity when compared with the ECU activity, we calculated the EMG ratio. Here, we simply divided the percent increase of FCR activity by that of ECU activity in the same arm. This was done for each task and in each participant separately, and we calculated the mean EMG ratio in each task across participants for the right and left arm separately (Fig. 2B). We conducted a one-sample *t*-test if the EMG ratio was significantly different from 1 (= FCR activity was equal to ECU activity). Finally, we examined the relationship between the maximum illusory angle and EMG ratio in the right arm during the tendon-vibration epoch across participants (Fig. 2C).

2.6. fMRI experiment

A 3.0 T SIEMENS scanner (MAGNETOM Allegra) with a bird cage head-coil provided T1-weighted anatomical images (3D-SPGR) and functional T2*-weighted echoplanar images (64 × 64 matrix, 3.0 mm × 3.0 mm, TE 40 msec). A functional image volume comprised of 44 3-mm-thick slices was imaged, which ensured that the whole brain was within the 192-mm × 192-mm field of view. The same 19 blindfolded participants rested comfortably in the supine position in the MR scanner. Both the right and left arms were naturally semi-pronated and extended in front of them, and fixed on wooden apparatuses as in the behavioral experiment (Fig. 1B).

The participants completed two vibration sessions and two execution-imagery sessions. As in the behavioral experiment, the tendon-vibration, bone-vibration, or rest epoch was repeated three times in the vibration session, and the execution, imagery, or rest epoch was also repeated three times in the execution-imagery session in a pseudo-randomized manner across participants (see above). The task required in each epoch and temporal organization of the experimental epoch in each session were identical to those performed in the behavioral experiment. We collected nine functional image volumes for each 27-sec epoch for each participant (TR = 3 sec). Eventually, a total of 101 volumes were collected in each session, including a 6-sec pre-session period, eight 6-sec inter-epoch-interval periods, and a 6-sec post-session period. In addition to these images, we also collected five functional images before each session to allow for magnetization equilibrium that were excluded from the analysis. During fMRI scanning, we did not measure EMG activity. The experimenter visually confirmed the successful performance of wrist movement during the execution epochs. As for the imagery epochs, we asked the participants if they could imagine that they actually performed the wrist movement after each execution-imagery session. All of them reported that they could do so as in the behavioral experiment.

2.7. Evaluation of illusory experience after scanning

As in the behavioral experiment, after each vibration session, we asked the participants if they experienced the illusion. All of the participants experienced the illusion in the tendon-vibration epochs, while none of them experienced any reliable illusions in the bone-vibration epochs. As in the behavioral experiment, after each vibration session, we asked the participants to flex their right wrists until they showed the maximum illusory flexion angle that was experienced in each of the three tendon-vibration epochs. We measured these angles from the relaxed position with the protractor (Fig. 1A) and calculated the mean maximum illusory angle across all six tendon-vibration epochs in two sessions for each participant.

2.8. fMRI data analysis

The fMRI data was analyzed with Statistical Parametric Mapping software (SPM8; http://www.fil.ion.ucl.ac.uk/spm; the Wellcome Department of Cognitive Neurology, London). The functional images were realigned to correct for head movements, coregistered with each participant's anatomical MRI, and transformed (by linear and non-linear transformation) to the format of the Montréal Neurological Institute (MNI) standard brain. The functional images were then spatially smoothed with a 4-mm full width at half maximum (FWHM) isotropic Gaussian kernel.

After the preprocessing, we fit a linear regression (general linear) model to the data obtained from each participant. As a vibration session, we prepared separate regressors for the tendon-vibration epochs and bone-vibration epochs. Likewise, separate regressors were prepared for execution epochs, imagery epochs, and rest epochs in an execution-imagery session. Each epoch was modeled with boxcar functions convolved with the canonical hemodynamic response function in SPM8. Thus, the regressors specified each epoch period with a hemodynamic delay in each session. To identify brain regions active during illusion, we contrasted tendon-vibration versus bone-vibration. Here, we could evaluate the effect of tendon-vibration (processing of muscle afferent input that elicits illusion) by subtracting the effect of vibration beside the tendon during bone-vibration (Naito et al., 2007, 2005). To depict brain regions active during execution and during imagery, we contrasted execution versus rest and imagery versus rest. Here, we could evaluate the effects of execution and imagery by removing the effect generated by listening to the pacing sounds (see above). These contrast images were generated for each participant separately. To evaluate inter-participant variability, the contrast images from all participants were entered into a random effect group analysis (second-level analysis; Friston, Holmes, & Worsley, 1999). A one-sample *t*-test was used (df = 18).

First, we performed whole brain analysis to depict the general feature of brain activations during each task (illusion, execution, and imagery). A voxel-wise threshold of $p < .001$ uncorrected was used to generate a cluster image and the significance in spatial extent of active-voxel clusters was evaluated ($p < .05$ family-wise error (FWE) corrected). As for the anatomical identification of active brain regions, we referred to the cytoarchitectonic probability maps in the MNI standard brain of the SPM anatomy toolbox v1.8 (Eickhoff et al., 2005). The results are tabulated in Tables 1–3.

2.9. Flip analysis

We further examined whether we can observe right-hemisphere dominance in frontoparietal activations during illusion by performing a flip analysis (Hagura et al., 2009; Naito & Ehrsson, 2006). The purpose of this analysis was to check whether the right-side dominance is confined to illusion (not observed during execution or imagery). First, the contrast image (e.g., tendon-vibration *vs* bone-vibration) in each participant was flipped (a left-to-right transformation on the *x*-axis) to make a left-right reversed image (flipped image). Then, we contrasted the original image with its flipped image for each participant. We know from our previous studies that we may reliably depict brain regions showing greater activity in one (either left or right) hemisphere than in the other by examining this contrast (Hagura et al., 2009; Naito & Ehrsson, 2006), even though the present flip method might not be a perfect approach, as the left and right hemispheres are not completely mirror images even after normalization of the individual brain to the standard brain (Shulman et al., 2010). The images (original image *vs* flipped

Table 1 – Brain activations during illusion (tendon *vs* bone).

	Clusters	Cluster size (voxels)	MNI coordinates of local maxima			T-value	Anatomical identification (most probable cytoarchitectonic area)
			x	y	z		
Left hemisphere							
Cortical	Insular cluster	255	−36	24	0	5.86	Anterior insula lobe
			−46	12	−2	5.20	Anterior insula lobe
			−54	8	0	4.6	Anterior insula lobe
	M1 cluster	82	−34	−24	58	5.63	*M1 (area 4a)
			−34	−24	48	3.87	*M1 (area 4p)
Subcortical	Caudate cluster	91	−18	6	18	5.83	Caudate
			−10	−8	18	4.57	Caudate
			−14	8	4	3.81	Caudate
Right hemisphere							
Cortical	Area 44-insular cluster	631	60	14	2	6.06	**Inferior frontal gyrus (area 44)
			36	20	−4	5.96	Anterior insula lobe
			46	12	−4	5.75	Anterior insula lobe
	Inferior parietal cluster	375	56	−44	46	7.28	**Inferior parietal lobule (area PFm)
			62	−34	46	5.68	**Supramarginal gyrus
			64	−24	40	5.46	Anterior supramarginal gyrus (area PFt)
	Middle frontal cluster	153	42	44	28	5.17	Middle frontal gyrus
			44	32	18	4.90	Inferior frontal gyrus (area 45)
			32	46	32	4.32	Middle frontal gyrus
	Orbitofrontal cluster	143	44	50	−2	5.54	Middle orbital gyrus
			44	40	−4	4.48	Inferior frontal gyrus (orbitalis)

Peaks more than 8 mm apart from each other were reported.
For anatomical identification of peaks, we only considered cytoarchitectonic areas with more than 30% probability available in the anatomy toolbox. The cytoarchitectonic area with the highest probability was reported for each peak. When cytoarchitectonic areas with more than 30% probability were not available for a peak, we simply provided its anatomical location. Single asterisk (*) indicates left-dominant activity and double asterisks (**) indicate right-dominant activity revealed by flip analysis.

image) obtained from all participants were entered into a second-level random effect group analysis. The same voxel-wise threshold of $p < .001$ uncorrected was used to generate a cluster image and the significance in spatial extent of active-voxel clusters was evaluated ($p < .05$ FWE corrected). Here, we used the original image (tendon-vibration *vs* bone-vibration) with a voxel-wise threshold of $p < .05$ uncorrected as an inclusive mask. This mask image allowed us to liberally specify brain regions where the activity at least increased during tendon-vibration, i.e., during illusion, when compared with bone-vibration. By using this mask image, we may identify hemispherically dominant activation within brain regions where activity increased during tendon-vibration by eliminating the possibility that the activation is fake due to deactivation in the corresponding brain region in an opposite hemisphere.

The same series of analyses were also done for the contrast images (execution *vs* rest and imagery *vs* rest).

2.10. *Region-of-interest (ROI) analysis*

The most important question in the present study is whether the right inferior frontoparietal cortices likely active during illusion belong to the large-scale inferior frontoparietal network connected by the inferior branch of the SLF (SLF III). In order to examine the involvement of brain regions connected by SLF fiber tracts in the illusion, execution, and imagery of right hand movement, we used probability maps of SLF fibers, which were obtained by elaborated methods to depict SLF fibers (SLF I, II, or III) with high quality (Rojkova et al., in press; Thiebaut de Schotten et al., 2012; http://sourceforge.net/projects/tractotron/files/).

Each map describes each branch of SLF (SLF I, II, or III) in each hemisphere. This was generated from diffusion tensor imaging tractography with a spherical deconvolution technique obtained from 47 normal volunteers (ages ranging from 22 to 71) that was normalized into the MNI standard brain. Thus, each map describes the stream of fiber tract and its connecting cortical regions of each SLF fiber in a probabilistic way. We set a threshold of .5. This gave us an image that describes both the fiber tract in the white matter and its connecting gray-matter cortical regions with a probability that a given fiber exists in over 50% of the 47 people. Thus, we think that these maps can be used as strong indicators, allowing us to describe the most probable location of brain activations in relation to cortical regions connected by SLF fibers, though these maps were not obtained from the present participants. As described in the Introduction, the SLF III appears to connect a wide range of inferior frontoparietal cortices. Indeed, when we examined the 50% probability map in relation to anatomical landmarks and the cytoarchitectonic probability maps, we found the SLF III fiber in the right hemisphere seems to connect the cortices lining postcentral sulcus including cytoarchitectonic area 2, intraparietal sulcus including cytoarchitectonic area IP1, inferior parietal lobules including cytoarchitectonic areas PF and its subregions, posterior parietal cortices including cytoarchitectonic areas PG/PGa,

Table 2 – Brain activations during execution (execution *vs* rest).

	Clusters	Cluster size (voxels)	MNI coordinates of local maxima			T-value	Anatomical identification (most probable cytoarchitectonic area)
			x	y	z		
Left hemisphere							
Cortical	PMd-SM1 cluster	1394	−30	−26	62	10.14	*M1 (area 4a)
			−34	−20	68	9.90	*PMD (area 6)
			−36	−40	68	6.7	*SI (area 1)
	SMA cluster	793	−4	−4	54	10.92	*SMA (area 6)
			−4	−2	66	7.20	SMA (area 6)
			−4	−12	50	6.33	*SMA (area 6)
	Inferior parietal cluster	397	−48	−26	18	10.26	*Parietal operculum (area OP1)
			−50	−36	22	4.80	Inferior supramarginal gyrus (area PFcm)
	Inferior frontal cluster	154	−48	0	4	7.06	Rolandic operculum
			−40	−4	18	4.41	Insula lobe
Subcortical	Thalamus-putamen cluster	1866	−16	−10	12	10.08	Thalamus
			−16	−20	12	8.63	*Thalamus
			−8	−20	6	8.37	Thalamus
			−32	−10	0	5.41	*Caudal putamen
Right hemisphere							
Cortical	Inferior parietal cluster	144	60	−30	22	5.26	Inferior supramarginal gyrus (area PFcm)
			50	−26	20	5.14	Parietal operculum (area OP1)
	Insular cluster	137	48	6	0	7.83	Insula lobe
Subcortical	Cerebellar cluster	1447	20	−48	−22	9.35	**Lobule VI
			8	−56	−10	7.76	**Lobule V
			30	−46	−28	7.18	**Lobule VI
		277	18	−64	−46	7.83	**Lobule VIIIA
			28	−52	−50	6.10	**Lobule VIIIA
			24	−60	−50	5.76	**Lobule VIIIA

Peaks more than 8 mm apart from each other were reported.
For anatomical identification of peaks, we only considered cytoarchitectonic areas with more than 30% probability available in the anatomy toolbox. The cytoarchitectonic area with the highest probability was reported for each peak. When cytoarchitectonic areas with more than 30% probability were not available for a peak, we simply provided its anatomical location. Single asterisk (*) indicates left-dominant activity and double asterisks (**) indicate right-dominant activity revealed by flip analysis.

Table 3 – Brain activations during imagery (imagery *vs* rest).

	Clusters	Cluster size (voxels)	MNI coordinates of local maxmima			T-value	Anatomical identification (most probable cytoarchitectonic area)
			x	y	z		
Left hemisphere							
Cortical	SMA cluster	225	−4	−2	56	6.92	SMA (area 6)
	Inferior parietal cluster	151	−54	−30	36	4.76	Inferior parietal lobule (area PF)
			−54	−36	30	4.52	Inferior supramarginal gyrus (area PFcm)
			−64	−34	38	4.10	Inferior parietal lobule (area PF)
	PMv cluster	107	−36	−6	44	4.66	PMv (area 6)
			−28	−8	48	4.4	PMv (area 6)
Subcortical	Putamen-thalamus cluster	630	−18	−8	10	5.76	Putamen
			−30	−4	0	5.68	Putamen
			−22	2	6	5.46	Globus pallidus
			−14	−4	10	4.54	Thalamus
Right hemisphere							
Subcortical	Putamen cluster	226	30	0	2	5.44	Putamen
			24	−4	14	5.20	Putamen
			22	4	4	4.44	Globus pallidus

Peaks more than 8 mm apart from each other were reported.
For anatomical identification of peaks, we only considered cytoarchitectonic areas with more than 30% probability available in the anatomy toolbox. The cytoarchitectonic area with the highest probability was reported for each peak. When cytoarchitectonic areas with more than 30% probability were not available for a peak, we simply provided its anatomical location. Single asterisk (*) indicates left-dominant activity and double asterisks (**) indicate right-dominant activity revealed by flip analysis.

parietal operculum including cytoarchitectonic area OP1, ventral part of cytoarchitectonic area 6, inferior frontal gyrus including cytoarchitectonic areas 44 and 45, middle frontal gyrus and middle orbital gyrus.

If brain activations during a task (illusion, execution, or imagery) form active-voxel clusters with significance spatial extent within a certain SLF map, we may consider that the task utilized a significant amount of neuronal resources in the brain regions connected by the SLF fiber. We then evaluated the significance of brain activations in terms of their spatial extent ($p < .05$ FWE corrected) within each probability map for SLF I, II, or III in each hemisphere (ROI). For this evaluation, we used an image for each task at a voxel-wise threshold of $p < .001$ uncorrected obtained from the second-level group analysis. The results are tabulated in Table 4.

2.11. *Correlation between amount of illusion and brain activity*

Finally, we examined whether the right-sided frontoparietal activity in the SLF III regions reflects the amount of illusion experienced by the participants. As described, we calculated the mean maximum illusory angle across all six tendon-vibration epochs from two sessions for each participant. These individual values were used as covariates in the second-level group analysis. We first depicted regions in the entire brain where activity correlated with the amount of illusion experienced by the participants. We generated a cluster image at the voxel-wise threshold of $p < .001$ uncorrected. From this analysis, we only found two active-voxel clusters in the right inferior frontoparietal regions in the entire brain space. These frontoparietal regions corresponded to those showing right-dominant activity during illusion (tendon-vibration *vs* bone-vibration). Finally, we performed small volume correction to evaluate the significance in the spatial extent of each cluster ($p < .05$ FWE corrected) within a 16-mm-radius sphere around a voxel of (60, −38, 46) and (52, −22, 6), respectively. The former had MNI coordinates (x, y, z) for a peak of the right-side dominant inferior parietal activation and the latter represented a peak of the right-side dominant inferior frontal activation, both of which were revealed by the flip analysis for illusion.

Table 4 – Brain activations in SLF I, II, III regions.

Condition	Cluster	Cluster size (voxels)	MNI coordinates of local maxima			T-value	Anatomical identification (most probable cytoarchitectonic area)
			x	y	z		
SLF I							
Left hemisphere							
Execution	SMA-CMA cluster	370	−4	−4	54	10.92	SMA (area 6)
			−4	−2	66	7.2	SMA (area 6)
			−12	−22	46	5.54	CMA (area 6)
	PMd-SM1 cluster	157	−22	−12	64	5.59	PMd (area 6)
			−26	−20	46	5.25	M1 (area 4p)
			−26	−28	50	4.88	SI (area 3a)
Imagery	SMA cluster	148	−4	−2	56	6.92	SMA (area 6)
SLF II							
Left hemisphere							
Execution	PMd-SM1 cluster	437	−38	−6	56	6.47	PMd (area 6)
			−34	−26	52	6.07	M1 (area 4p)
			−38	−36	64	5.78	SI (area 1)
SLF III							
Left hemisphere							
Execution	Inferior parietal cluster	189	−44	−28	20	9.75	Parietal operculum (area OP1)
Imagery	Inferior parietal cluster	137	−54	−30	36	4.76	Inferior parietal lobule (area PF)
			−54	−36	30	4.52	Inferior supramarginal gyrus (area PFcm)
			−62	−34	38	4.00	Inferior parietal lobule (area PF)
Right hemisphere							
Illusion	Inferior parietal cluster	253	56	−44	46	7.28	Inferior parietal lobule (area PFm)
			62	−34	46	5.68	Supramarginal gyrus
			48	−36	46	4.5	Anterior supramarginal gyrus (area PFt)
	Orbitofrontal cluster	136	44	50	−2	5.54	Middle orbital gyrus
			44	40	−4	4.48	Inferior frontal gyrus (orbitalis)
	Area 44 cluster	123	58	16	2	5.21	Inferior frontal gyrus (area 44)
			58	16	20	5.2	Inferior frontal gyrus (area 44)
			58	14	12	4.77	Inferior frontal gyrus (area 44)
	Area 45 cluster	78	44	32	18	4.9	Inferior frontal gyrus (area 45)

Peaks more than 8 mm apart from each other were reported.
For anatomical identification of peaks, we only considered cytoarchitectonic areas with more than 30% probability available in the anatomy toolbox. The cytoarchitectonic area with the highest probability was reported for each peak. When cytoarchitectonic areas with more than 30% probability were not available for a peak, we simply provided its anatomical location. Single asterisk (*) indicates left-dominant activity and double asterisks (**) indicate right-dominant activity revealed by flip analysis.

3. Results

3.1. Results from behavioral experiment outside scanner

In the execution-imagery session, we found a robust increase of EMG activity in the right arm in the execution epoch where the participants performed their wrist movements. When compared with the rest, both FCR and ECU activities increased with prominence in the former muscle (Fig. 2A). In contrast, in the imagery epoch where they imagined actually performing the wrist movement without generating any actual movements, no such robust EMG increase was observed in either muscle. The EMG ratio, which could describe the prominence of the FCR activity when compared with the ECU activity, was significantly different from 1 (= FCR activity was equal to ECU activity) for the execution epoch ($df = 18$, $t = 3.3$, $p < .005$; Fig. 2B), which was not the case in the imagery epoch ($p = .95$).

In the vibration session, when the participants experienced illusory flexion of the right stationary wrist in the tendon-vibration epoch, a slight increase in EMG activity was observed in both the right FCR and ECU muscles (Fig. 2A). The similar subtle EMG increase was also observed in the bone-vibration epoch even when no substantial illusory experiences were reported. When we examined the EMG ratio, we found no significant prominence of FCR activity for both epochs ($p > .2$). This means that, even when the participants experienced a fair amount of illusory flexion movement (29.2 ± 10.2°; mean ± SD across participants), the EMG activity in the agonistic muscle was as not robust as in the execution epoch. Indeed, when we examined the relationship between the amount of illusory flexion angle and the EMG ratio across participants, we found no significant correlation between these two variables ($N = 19$, $r = .3$, $p > .2$; Fig. 2C). A significant correlation was also not observed when we examined the relationship between the amount of illusion and the increase of EMG activity in each muscle separately ($r = -.1$ for ECU, $r = .26$ for FCR; not shown in figure). Hence, a substantial increase of EMG activity and an FCR-dominant EMG pattern were observed only during the execution of wrist movement. Even though the participants experienced illusory flexion, these were not observed during illusion.

EMG activities in the left FCR and ECU muscles were consistently silent in either epoch, meaning that the left hand was completely relaxed in every task.

3.2. Behavioral results in fMRI experiment

In the execution epoch, we visually checked that all participants generated their wrist movements in synchronization with the sounds. In contrast, no overt hand movements were observed in the imagery epoch, though most of the participants reported that they could imagine their wrist movements at the same pace as if they actually performed them.

In the vibration session, no overt hand movements were observed both in the tendon-vibration and bone-vibration epochs. When we asked them after each session, all participants reported that they experienced the illusory flexion in the tendon-vibration epoch, while no substantial illusions were experienced in the bone-vibration epoch. In the tendon-vibration epoch, the participants experienced illusory flexion movement amounts comparable to the behavioral experiment (24.2 ± 7.5°; mean ± SD across participants). When we evaluated the relationship between the mean maximum illusory angle obtained in the behavioral experiment and that in the fMRI experiment across participants, we found a significant correlation across participants ($r = .68$, $df = 17$, $p < .01$; not shown in figure). This indicated that illusory experience was highly replicable in the sense that a participant who felt larger degree of illusory wrist flexion outside the scanner (in the behavioral experiment) also experienced relatively larger degree of illusion inside the scanner.

3.3. Brain activations in the entire brain

When we depicted brain regions active during illusion (tendon-vibration *vs* bone-vibration), we found that the primary motor cortex (M1: cytoarchitectonic areas 4a and 4p), dorsal premotor cortex (PMd), anterior insular cortices, caudate nucleus, and ventrolateral thalamus activated in the left hemisphere (Fig. 3A, B). In the right hemisphere (Fig. 3B, C), illusion activated the inferior frontoparietal cortices including the inferior frontal gyrus (cytoarchitectonic areas 44 and 45), anterior insular cortex, middle frontal gyrus, orbitofrontal cortex, and inferior parietal cortices (cytoarchitectonic areas PFm and PFt). Flip analysis revealed right-side dominance of the inferior frontoparietal activities (areas 44 and PFm) in addition to the left-side dominance of M1/PMd activity. These results are tabulated in Table 1.

During execution (execution *vs* rest), the contralateral (left) primary sensory-motor cortices (SM1) and secondary motor areas activated (Fig. 3A, B). These included M1, PMd, primary somatosensory cortex (SI), supplementary motor area (SMA), and caudal part of the cingulate motor area (CMA). The SMA activity also extendeds into the right hemisphere. In addition to these motor areas, execution also activated the inferior frontoparietal cortices including the frontal operculum, insular cortex, and inferior parietal cortex (cytoarchitectonic areas OP1 and PFcm) in the left hemisphere. Furthermore, we found subcortical activation in the left thalamus, caudal part of the putamen, and brain stem. The thalamic activity also extended into the right hemisphere. In the right hemisphere, the inferior frontoparietal cortices including the insular cortex and inferior parietal cortex (cytoarchitectonic areas OP1 and PFcm) activated (Fig. 3C). Finally, we also identified activations in the right cerebellum (lobules V, VI, VIIB, and VIIIA). Flip analysis revealed left-side dominance of activities in the SM1, SMA, CMA, area OP1, thalamus, and putamen and the right-side dominance was only observed in the cerebellar activities (lobules V, VI, VIIB, and VIIIA). The results are tabulated in Table 2.

Imagery (imagery *vs* rest) activated the contralateral (left) secondary motor areas (SMA, PMd, and ventral premotor cortex: PMv; Fig. 3A, B). The inferior parietal cortex (cytoarchitectonic areas PF and PFcm), putamen, and thalamus also activated in the left hemisphere. In the right hemisphere, only the right putamen activated during imagery.

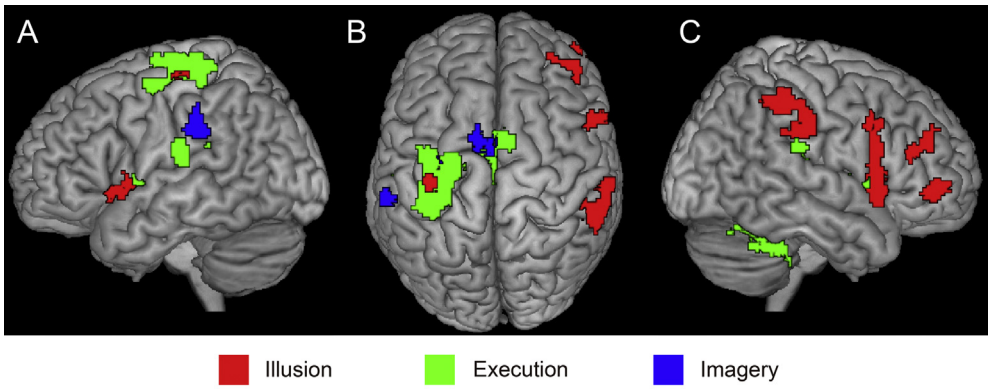

Fig. 3 – Brain regions active during illusion (red), execution (green), and imagery (blue). Brain activations are superimposed onto the MNI standard brain in the left lateral view (A), top view (B), and the right lateral view (C). Different qualities across the three motor-related events are reflected as distinct brain activation patterns in the entire brain. Illusion predominantly activated the frontoparietal cortices in the right hemisphere. Details of the anatomical location of brain activations are described in Tables 1–3

Flip analysis revealed no lateralized brain activity during imagery. The results are tabulated in Table 3.

Viewed collectively, the right-side dominance of inferior frontoparietal activities was confined to illusion, though execution also activated the right inferior frontoparietal cortices.

3.4. *Brain activations in SLF I, II, and III*

When we evaluated the involvement of brain regions connected by SLF I, II, and III in each task, we found clear functional segregation between illusion and the other two tasks. Namely, during illusion, significant activations were only observed in the right SLF III regions, while during execution and imagery, these were only identified in the left SLF regions (Table 4 and Fig. 4).

The activations during illusion were located in the inferior frontal cortices (cytoarchitectonic areas 44 and 45), middle frontal gyrus, orbitofrontal cortex, and inferior parietal cortices (areas PFm and PFt) in the right cerebral regions connected by the SLF III (Fig. 4H, I). Importantly, the inferior frontoparietal regions where we observed right-side dominant activity (see above) belonged to the SLF III regions (not shown in figure). No significant activations were observed either in the left SLF III regions or in the regions connected by SLF I and II of both hemispheres.

In contrast, no significant activations were observed in the right SLF III regions during execution and imagery (Fig. 4H, I). During execution, we found significant activations in SMA, CMA, (area 6), the medial aspects of PMd (area 6), and SM1 (areas 4p and 3a), which belong to the left SLF I regions (Fig. 4A, B). We also found significant activations in the lateral aspects of PMd (area 6) and SM1 (areas 4p and 1) that belong to the left SLF II regions (Fig. 4D, E). Finally, we also found significant activation in the parietal operculum (area OP1) of the left SLF III regions (Fig. 4G). During imagery, we found significant activations in the SMA (area 6) of the left SLF I regions (Fig. 4B) and in the inferior parietal cortices (areas PF and PFcm) of the left SLF III regions (Fig. 4G, H).

3.5. *Right inferior frontoparietal activity correlated with the amount of illusion*

When we examined whether the right-side dominant activities in the inferior frontoparietal cortices reflect the amount of illusion experienced by the participants, we found that activities in area 45 (x, y, z coordinates = 56, 18, 24) and area PF (58, −38, 32) of the right hemisphere correlated well with the amount of illusion across participants ($p = .89$ and $p = .79$, respectively) (Fig. 5). The number of voxels forming a cluster in each area was 19 and 16, respectively. These clusters belonged to the right SLF III regions (Fig. 5A). These were the only clusters of active voxels in the entire brain and their significance in terms of cluster size was confirmed by the small volume correction (see Methods). This means that the participants who experienced larger degree of illusions showed greater activity in the right inferior frontoparietal cortices connected by the SLF III. This indicates that the degree of these activities may reflect kinesthetic illusory awareness.

4. Discussion

We showed that the right inferior frontoparietal regions connected by SLF III widely activated only during illusion. Among these regions, activities in the right inferior parietal cortices and inferior frontal cortices showed right-side dominance and correlated well with the amount of illusion experienced by the participants. These results indicate that the inferior frontoparietal network connected by SLF III, especially in the right hemisphere, plays predominant roles when people recognize postural change of their limbs during illusion.

4.1. *Comparison with previous illusion studies*

The present illusion task required the participants not only to experience illusory movement of the right hand, but also to memorize its maximum angle in order to replicate it after the scanning. Thus, the present task required more cognitive demands, such as kinesthetic working memory, which were not

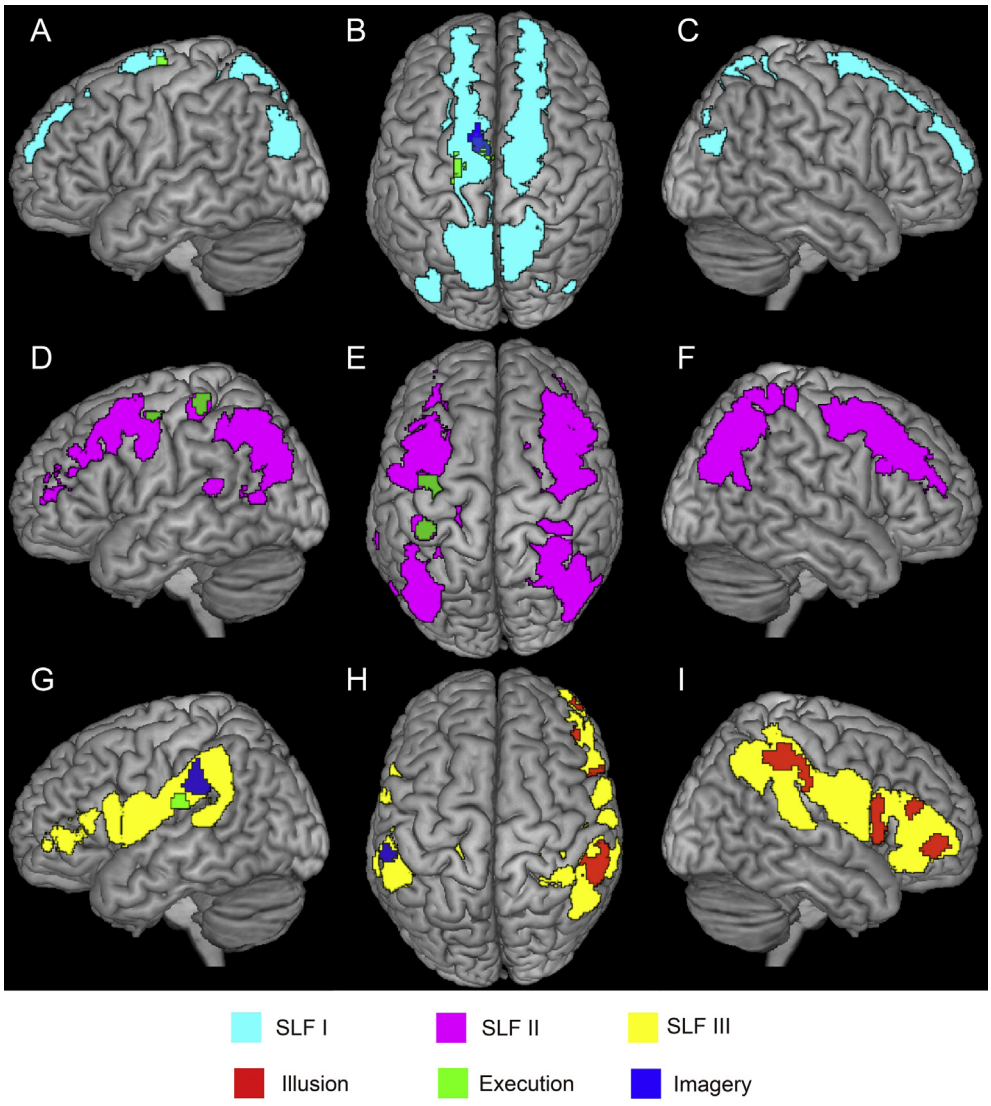

Fig. 4 – Brain activations during illusion (red), execution (green), and imagery (blue) in relation to brain regions connected by SLF I (cyan sections in panels A–C), II (magenta sections in panels D–F), and III (yellow sections in panels G–I). These are superimposed onto the MNI standard brain. Only illusion substantially recruited the SLF III regions in the right hemisphere (panels H and I), while execution and imagery widely recruited brain regions connected by SLF I, II, and III, but only in the left hemisphere. Details of the anatomical location of brain activations are described in Table 4.

explicitly required in our series of illusion studies (Naito, Ehrsson, Geyer, Zilles, & Roland, 1999; Naito, Kochiyama, et al., 2002; Naito et al., 2007; Naito, Roland, & Ehrsson, 2002; Naito et al., 2005). In line with this view, the present illusion task strongly activated the right middle frontal gyrus and orbitofrontal cortex, which was not consistently reported in our previous studies (see Supplementary Fig. 2). Thus, these frontal regions may, at least partly, contribute to memorizing (encoding) the kinesthetic experience and its associated cognitive (attentional) functions (cf. Hagen, Zald, Thornton, & Pardo, 2002). This view is corroborated by the finding that patients who have undergone large right frontal lobe excision have impaired performance in kinesthetic tasks, which requires monitoring of kinesthetic feedback in order to duplicate experienced arm movements, that was not observed in patients with left frontal lobe damage (Leonard & Milner, 1991).

In contrast, despite the differences in task demands and participants, the right inferior frontoparietal cortices active in the present illusion task fit well with those in our previous studies where blindfolded participants passively experienced the illusion (Naito et al., 2007, 2005; Supplementary Fig. 2). Thus, the right inferior frontoparietal activities during illusion were highly consistent across studies. The exact roles of the right inferior frontoparietal cortices are still unveiled (see also below). However, we know from our previous studies that (1) the right inferior frontoparietal activations largely overlap no matter when people experience illusory movement of the hand or foot on the right or left side (Naito et al., 2007, 2005) and (2) the right inferior frontoparietal cortices involve visuokinesthetic processing where people recognize postural change of the right hand by combining its visual and kinesthetic information (Hagura et al., 2009). These lines of evidence indicate that higher-order (supra-effector and

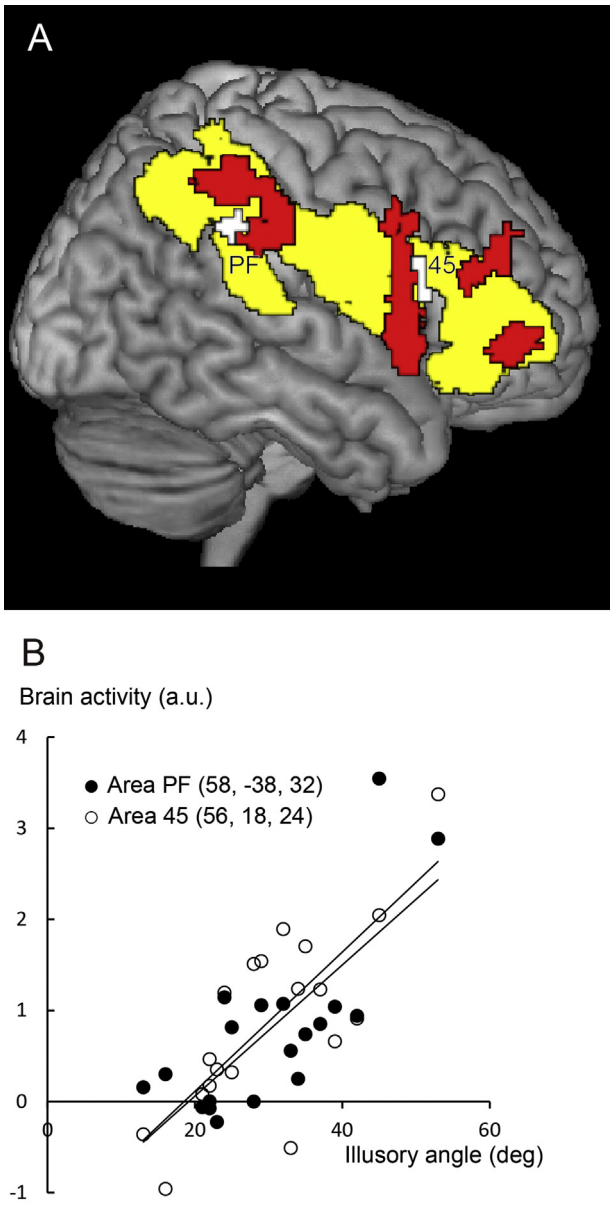

Fig. 5 – Correlation between the right inferior frontoparietal activities and illusory angle. A: Right inferior frontoparietal cortices active during illusion (red sections). White sections in areas PF and 45 show significant positive correlation with the illusory angle. The brain activities are rendered onto the MNI standard brain. Yellow sections indicate brain regions connected by the SLF III. B: Significant positive correlation between brain activity (vertical axis) and illusory angle (horizontal axis). Each dot represents data obtained from each participant. A filled dot represents data obtained from area PF of the inferior parietal cortex and an open dot represents data obtained from area 45 of the inferior frontal cortex.

multimodal) aspects of neuronal processing associated with kinesthetic illusion should take place in the right inferior frontoparietal cortices.

These features make clear the contrast with neuronal processing in the motor network active during illusion. We have consistently reported across studies that motor areas, especially M1/PMd, become active during illusion of hand, arm, or foot (Naito et al., 1999; Naito, Kochiyama, et al., 2002; Naito et al., 2011, 2007; Naito, Roland, et al., 2002; Naito et al., 2005). In the present study, we also confirmed the contralateral (left) M1/PMd activity, with absolutely no actual movements of the right hand and probably with no substantial increase of EMG activity during illusion (Fig. 2). In contrast to the frontoparietal cortices, the somatotopical sections in the motor areas basically become active during illusion and their possible role (at least in M1/PMd) is processing of kinesthetic input from the muscle spindle afferent recruited by tendon vibration (Colebatch, Sayer, Porter, & White, 1990) by covertly generating sub-threshold motor commands (Naito, 2004). If one considers the fact that the muscle spindle afferent is capable of signaling the direction and speed of a limb's movement (Burke, Gandevia, & Macefield, 1988; Burke, Hagbarth, Lofstedt, & Wallin, 1976; Edin & Vallbo, 1988, 1990; Ribot-Ciscar & Roll, 1998), we may assume that somatotopically organized M1/PMd activity during illusion may represent information about "which limb is moving toward which direction at which velocity." Thus, the fundamental elements bearing kinesthesia are likely processed in a M1/PMd-centered motor network during illusion.

In our previous studies, we showed that the degree of motor-cortical (M1/PMd) excitability is correlated with the amount of illusion (how much people experience illusory hand movement; Naito, Roland, et al., 2002). We also showed that the contralateral M1/PMd activity during illusion reduces in proportion to the degree of reduction in illusion attenuated by vision (how much illusion attenuates when people look at an immobile hand having illusory movement; Hagura et al., 2007). Furthermore, focal damage in M1/PMd may severely impair the illusory experience of a contralateral limb (Naito et al., 2011).

In the present study, we further provided new evidence that the right inferior frontoparietal activities may also reflect the amount of illusion (Fig. 5). This generally fits well with the previous finding that higher-intensity electrical stimulation to the human right inferior parietal cortex causes the illusory sensation of limb movement (Desmurget et al., 2009). This is direct evidence that right inferior parietal activity is capable of eliciting kinesthetic illusion. Together with the recent finding that a certain amount of brain activity in the right frontoparietal network is required to experience illusory limb movement (Cignetti et al., 2014), the right inferior frontoparietal network must also play a crucial role in experiencing kinesthetic illusion.

4.2. *Roles of right SLF III network during illusion*

SLF III seems to connect a wide range of inferior frontoparietal cortices including anterior parietal (higher-order somatic) cortices, posterior parietal (visual association) cortices, inferior parietal cortices, inferior frontal cortices, ventrolateral prefrontal cortices, and orbitofrontal cortices (Fig. 4H, I). Since the present illusion task broadly activated the brain regions connected by the right SLF III (Table 4 and Fig. 4H, I), kinesthetic illusory experience is supported by the large-scale brain network connected by the right SLF III.

During illusion, the brain receives and processes muscle afferent input from a vibrated hand, but the brain does not explicitly prepare and generate hand movement. In contrast, during execution, the brain prepares and executes hand movement and also receives and processes sensory afferent input from the moving hand. Finally, during imagery, the brain prepares and mentally simulates hand movement (Ehrsson, Geyer, & Naito, 2003; Naito & Sadato, 2003), but it does not receive and process veridical sensory afferent input from the hand. These different qualities across the three motor-related events were reflected as distinct brain activation patterns not only in the entire brain, but also in the brain regions connected by the SLF fibers (Figs. 3 and 4, and Table 4). Namely, only illusion recruited the SLF III regions in the right hemisphere (Fig. 4H, I, and Table 4), while execution and imagery widely recruited brain regions connected by SLF I, II, and III, but only in the left hemisphere (Fig. 4 and Table 4). Eventually, the right-side dominance of the inferior frontoparietal SLF III activities was confined to illusion (Table 3). These lines of evidence imply the functional asymmetry between two (right and left) frontoparietal cortices (c.f. Daprati et al., 2010).

Lacking of robust activations in the right inferior frontoparietal SLF III regions during execution and imagery (Fig. 3) indicates that these activations are less relevant to top-down motor processes such as intention, planning, preparation and generation of hand movement. Thus, the activations are associated with bottom-up but active-sensing processes where the brain recognizes postural change of our hand by largely relying on sensory afferent input. Even though the brain likely receives sensory input during execution, the brain can notice the occurrence of hand movement through the generation of motor commands without heavily relying on sensory afferent input. This could be one of the reasons why we observed the right-side activations only during illusion.

To experience postural change of our limb during illusion, the brain has to build-up and update the internal representation of spatial configuration (= postural model) of our limb by monitoring the current status of the musculoskeletal system. To build-up and update the postural model of our limb, the inferior frontal and inferior parietal cortices appear to be suitable, because one of the characteristics of these cells is to process information represented in the body-centered/body-part-centered reference frame (Graziano, Hu, & Gross, 1997; Ishida, Nakajima, Inase, & Murata, 2010). As for the monitoring function, it is known that human right inferior frontal damage may disrupt the self-monitoring function, which impairs the ability of people to appropriately evaluate the current status of the musculoskeletal motor system (Berti et al., 2005). This evidence suggests involvement of the inferior frontoparietal SLF III network in the series of neuronal computation.

Furthermore, in order for the brain to monitor, build-up, and update the postural model of our limb, which momentarily changes, speedy processing of every fresh sensory information pertaining to our limb is necessary. In this sense, the anatomical character of the right SLF III seems to be suitable. Namely, the volume of SLF III in the right hemisphere has been shown to be significantly greater than that in the left hemisphere (Thiebaut de Schotten et al., 2011; see also Fig. 4G–I). This could be explained by many possible factors, e.g., the right SLF III may contain a greater number of axons, axons with a thicker diameter, richer myelinated axons, and so on. However, all of these possibilities commonly suggest advantageously speedy neuronal processing by the right SLF III.

Viewed collectively, we propose that the right inferior frontoparietal SLF III network active during illusion may bear the series of functions of monitoring, building-up, and updating the postural model of our limb, i.e., body schema (Head & Holmes, 1911). To evaluate the current status of the musculoskeletal system, this network most probably communicates with the motor network that processes fundamental elements for kinesthesia. The inferior frontoparietal SLF III network appears to be suitable for the series of neuronal processing, owing to its higher capability of speedy multisensory processing of neuronal information represented in the body-centered/body-parts-centered coordinate system. Together with the finding that the right inferior frontoparietal activities reflect the degree of kinesthetic illusory awareness (Fig. 5), we assume that corporeal awareness of kinesthetic illusory experience is an attribute of neuronal activities in the right inferior frontoparietal SLF III network where the brain builds-up and updates the postural model of our limb (c.f. Kinsbourne, 2006).

In the present study, we merely showed right-side dominance of the human frontoparietal cortices in just one example of corporeal awareness, i.e., kinesthetic illusion. However, the right hemisphere dominance has been reported in a wider range of tasks (e.g., self-face recognition task: Devue & Bredart, 2011; Keenan, Wheeler, Gallup, & Pascual-Leone, 2000; Morita et al., 2008; Sugiura et al., 2006). These imply the further possibility that the right-side large-scale SLF III network also plays essential roles in broader types of corporeal awareness, which can be a basis for conscious experience of the physical self.

5. Conclusion

In the present study, we found that only illusion predominantly activated the right inferior frontoparietal regions connected by SLF III which were not substantially recruited during execution and imagery. This right hemisphere dominance was only observed when participants experienced kinesthetic illusion and the right frontoparietal activities correlated well with the amount of kinesthetic illusory awareness.

The results of the present study depicted that the key role of the right inferior frontoparietal network connected by SLF III in corporeal awareness.

Acknowledgment

This work was supported by Scientific Research on Innovative Areas “Embodied-brain” (JSPS KAKENHI No. 26120003) to author EN, by Grant-in-Aid for Specially Promoted Research (No. 24000012) to EN, Grant-in-Aid for Young Scientists B (No. 26870933) to KA, and Grant-in-Aid for JSPS Fellows to KA.

Supplementary data

Supplementary data related to this article can be found at http://dx.doi.org/10.1016/j.cortex.2016.01.017.

REFERENCES

Berlucchi, G., & Aglioti, S. (1997). The body in the brain: neural bases of corporeal awareness. *Trends in Neurosciences, 20*(12), 560–564.

Berti, A., Bottini, G., Gandola, M., Pia, L., Smania, N., Stracciari, A., et al. (2005). Shared cortical anatomy for motor awareness and motor control. *Science, 309*(5733), 488–491.

Binder, J. R., Frost, J. A., Hammeke, T. A., Cox, R. W., Rao, S. M., & Prieto, T. (1997). Human brain language areas identified by functional magnetic resonance imaging. *The Journal of Neuroscience, 17*(1), 353–362.

Burke, D., Gandevia, S. C., & Macefield, G. (1988). Responses to passive movement of receptors in joint, skin and muscle of the human hand. *The Journal of Physiology, 402*(1), 347–361.

Burke, D., Hagbarth, K. E., Lofstedt, L., & Wallin, B. G. (1976). The responses of human muscle spindle endings to vibration of non-contracting muscles. *The Journal of Physiology, 261*(3), 673–693.

Catani, M., Allin, M. P., Husain, M., Pugliese, L., Mesulam, M. M., Murray, R. M., et al. (2007). Symmetries in human brain language pathways correlate with verbal recall. *Proceedings of the National Academy of Sciences of the United States of America, 104*(43), 17163–17168.

Cignetti, F., Vaugoyeau, M., Nazarian, B., Roth, M., Anton, J. L., & Assaiante, C. (2014). Boosted activation of right inferior frontoparietal network: a basis for illusory movement awareness. *Human Brain Mapping, 35*(10), 5166–5178.

Colebatch, J. G., Sayer, R. J., Porter, R., & White, O. B. (1990). Responses of monkey precentral neurones to passive movements and phasic muscle stretch: relevance to man. *Electroencephalography and Clinical Neurophysiology, 75*(2), 44–55.

Daprati, E., Sirigu, A., & Nico, D. (2010). Body and movement: consciousness in the parietal lobes. *Neuropsychologia, 48*(3), 756–762.

Desmurget, M., Reilly, K. T., Richard, N., Szathmari, A., Mottolese, C., & Sirigu, A. (2009). Movement intention after parietal cortex stimulation in humans. *Science, 324*(5928), 811–813.

Devue, C., & Bredart, S. (2011). The neural correlates of visual self-recognition. *Consciousness and Cognition, 20*(1), 40–51.

Edin, B. B., & Vallbo, A. B. (1988). Stretch sensitization of human muscle spindles. *The Journal of Physiology, 400*(1), 101–111.

Edin, B. B., & Vallbo, A. B. (1990). Dynamic response of human muscle spindle afferents to stretch. *Journal of Neurophysiology, 63*(6), 1297–1306.

Ehrsson, H. H., Geyer, S., & Naito, E. (2003). Imagery of voluntary movement of fingers, toes, and tongue activates corresponding body-part-specific motor representations. *Journal of Neurophysiology, 90*(5), 3304–3316.

Eickhoff, S. B., Stephan, K. E., Mohlberg, H., Grefkes, C., Fink, G. R., Amunts, K., et al. (2005). A new SPM toolbox for combining probabilistic cytoarchitectonic maps and functional imaging data. *NeuroImage, 25*(4), 1325–1335.

Friston, K. J., Holmes, A. P., & Worsley, K. J. (1999). How many subjects constitute a study? *NeuroImage, 10*(1), 1–5.

Goodwin, G. M., McCloskey, D. I., & Matthews, P. B. (1972). Proprioceptive illusions induced by muscle vibration: contribution by muscle spindles to perception? *Science, 175*(4028), 1382–1384.

Graziano, M. S., Hu, X. T., & Gross, C. G. (1997). Visuospatial properties of ventral premotor cortex. *Journal of Neurophysiology, 77*(5), 2268–2292.

Hagen, M. C., Zald, D. H., Thornton, T. A., & Pardo, J. V. (2002). Somatosensory processing in the human inferior prefrontal cortex. *Journal of Neurophysiology, 88*(3), 1400–1406.

Hagura, N., Oouchida, Y., Aramaki, Y., Okada, T., Matsumura, M., Sadato, N., et al. (2009). Visuokinesthetic perception of hand movement is mediated by cerebro-cerebellar interaction between the left cerebellum and right parietal cortex. *Cerebral Cortex, 19*(1), 176–186.

Hagura, N., Takei, T., Hirose, S., Aramaki, Y., Matsumura, M., Sadato, N., et al. (2007). Activity in the posterior parietal cortex mediates visual dominance over kinesthesia. *The Journal of Neuroscience, 27*(26), 7047–7053.

Head, H., & Holmes, G. (1911). Sensory disturbances from cerebral lesions. *Brain, 34*(2–3), 102–254.

Ishida, H., Nakajima, K., Inase, M., & Murata, A. (2010). Shared mapping of own and others' bodies in visuotactile bimodal area of monkey parietal cortex. *Journal of Cognitive Neuroscience, 22*(1), 83–96.

Keenan, J. P., Wheeler, M. A., Gallup, G. G., Jr., & Pascual-Leone, A. (2000). Self-recognition and the right prefrontal cortex. *Trends in Cognitive Sciences, 4*(9), 338–344.

Kinsbourne, M. (2006). From unilateral neglect to the brain basis of consciousness. *Cortex, 42*(6), 869–874.

Kito, T., Hashimoto, T., Yoneda, T., Katamoto, S., & Naito, E. (2006). Sensory processing during kinesthetic aftereffect following illusory hand movement elicited by tendon vibration. *Brain Research, 1114*(1), 75–84.

Leonard, G., & Milner, B. (1991). Contribution of the right frontal lobe to the encoding and recall of kinesthetic distance information. *Neuropsychologia, 29*(1), 47–58.

Makris, N., Kennedy, D. N., McInerney, S., Sorensen, A. G., Wang, R., Caviness, V. S., Jr., et al. (2005). Segmentation of subcomponents within the superior longitudinal fascicle in humans: a quantitative, in vivo, DT-MRI study. *Cerebral Cortex, 15*(6), 854–869.

Melzack, R. (1990). Phantom limbs and the concept of a neuromatrix. *Trends in Neurosciences, 13*(3), 88–92.

Morita, T., Itakura, S., Saito, D. N., Nakashita, S., Harada, T., Kochiyama, T., et al. (2008). The role of the right prefrontal cortex in self-evaluation of the face: a functional magnetic resonance imaging study. *Journal of Cognitive Neuroscience, 20*(2), 342–355.

Naito, E. (1994). Controllability of motor imagery and transformation of visual imagery. *Perceptual and Motor Skills, 78*(2), 479–487.

Naito, E. (2004). Sensing limb movements in the motor cortex: how humans sense limb movement. *Neuroscientist, 10*(1), 73–82.

Naito, E., & Ehrsson, H. H. (2006). Somatic sensation of hand-object interactive movement is associated with activity in the left inferior parietal cortex. *The Journal of Neuroscience, 26*(14), 3783–3790.

Naito, E., Ehrsson, H. H., Geyer, S., Zilles, K., & Roland, P. E. (1999). Illusory arm movements activate cortical motor areas: a positron emission tomography study. *The Journal of Neuroscience, 19*(14), 6134–6144.

Naito, E., Kochiyama, T., Kitada, R., Nakamura, S., Matsumura, M., Yonekura, Y., et al. (2002). Internally simulated movement sensations during motor imagery activate cortical motor areas and the cerebellum. *The Journal of Neuroscience, 22*(9), 3683–3691.

Naito, E., Matsumoto, R., Hagura, N., Oouchida, Y., Tomimoto, H., & Hanakawa, T. (2011). Importance of precentral motor

regions in human kinesthesia: a single case study. *Neurocase, 17*(2), 133–147.
Naito, E., Nakashima, T., Kito, T., Aramaki, Y., Okada, T., & Sadato, N. (2007). Human limb-specific and non-limb-specific brain representations during kinesthetic illusory movements of the upper and lower extremities. *European Journal of Neuroscience, 25*(11), 3476–3487.
Naito, E., Roland, P. E., & Ehrsson, H. H. (2002). I feel my hand moving: a new role of the primary motor cortex in somatic perception of limb movement. *Neuron, 36*(5), 979–988.
Naito, E., Roland, P. E., Grefkes, C., Choi, H. J., Eickhoff, S., Geyer, S., et al. (2005). Dominance of the right hemisphere and role of area 2 in human kinesthesia. *Journal of Neurophysiology, 93*(2), 1020–1034.
Naito, E., & Sadato, N. (2003). Internal simulation of expected sensory experiences before movements get started. *Reviews in the Neurosciences, 14*(4), 387–399.
Ribot-Ciscar, E., & Roll, J. P. (1998). Ago-antagonist muscle spindle inputs contribute together to joint movement coding in man. *Brain Research, 791*(1–2), 167–176.
Rojkova, K., Volle, E., Urbanski, M., Humbert, F., Dell'Acqua, F., & Thiebaut de Schotten, M. Atlasing the frontal lobe connections and their variability due to age and education: a spherical deconvolution tractography study. *Brain Structure and Function* [in press].
Roll, J. P., & Vedel, J. P. (1982). Kinaesthetic role of muscle afferents in man, studied by tendon vibration and microneurography. *Experimental Brain Research, 47*(2), 177–190.
Roll, J. P., Vedel, J. P., & Ribot, E. (1989). Alteration of proprioceptive messages induced by tendon vibration in man: a microneurographic study. *Experimental Brain Research, 76*(1), 213–222.
Shulman, G. L., Pope, D. L., Astafiev, S. V., McAvoy, M. P., Snyder, A. Z., & Corbetta, M. (2010). Right hemisphere dominance during spatial selective attention and target detection occurs outside the dorsal frontoparietal network. *The Journal of Neuroscience, 30*(10), 3640–3651.
Springer, J. A., Binder, J. R., Hammeke, T. A., Swanson, S. J., Frost, J. A., Bellgowan, P. S., et al. (1999). Language dominance in neurologically normal and epilepsy subjects: a functional MRI study. *Brain, 122*(Pt 11), 2033–2046.
Sugiura, M., Sassa, Y., Jeong, H., Miura, N., Akitsuki, Y., Horie, K., et al. (2006). Multiple brain networks for visual self-recognition with different sensitivity for motion and body part. *NeuroImage, 32*(4), 1905–1917.
Thiebaut de Schotten, M., Dell'Acqua, F., Forkel, S. J., Simmons, A., Vergani, F., Murphy, D. G., et al. (2011). A lateralized brain network for visuospatial attention [Brief Communication] *Nature Neuroscience, 14*(10), 1245–1246.
Thiebaut de Schotten, M., Dell'Acqua, F., Valabregue, R., & Catani, M. (2012). Monkey to human comparative anatomy of the frontal lobe association tracts. *Cortex, 48*(1), 82–96.
Wada, J., & Rasmussen, T. (2007). Intracarotid injection of sodium amytal for the lateralization of cerebral speech dominance. 1960. *Journal of Neurosurgery, 106*(6), 1117–1133.